Available online at www.sciencedirect.com
SCIENCE DIRECT®
Control Engineering Practice 14 (2006) 833–842
CONTROL ENGINEERING PRACTICE
www.elsevier.com/locate/conengprac

Multivariable adaptive control of instabilities arising in jet engines ☆

Miroslav Krstic[a,*], Andrzej Banaszuk[b]

[a]Department of Mechanical and Aerospace Engineering, University of California, San Diego, La Jolla, CA 92093-0411, USA
[b]United Technologies Research Center, 411 Silver Lane, MS 129-15, East Hartford, CT 06108, USA

Received 20 September 2002; accepted 5 April 2005
Available online 13 June 2005

Abstract

We consider a class of MIMO LTI models with uncertain resonant modes and time delays, which are common in control of instabilities arising in jet engines. With uncertain delays preventing the use of model reference adaptive control, we develop an adaptive MIMO pole placement scheme for the system. We use indirect adaptation, estimating a small number of physical parameters from a nonlinearly parametrized plant. To address the highly noisy environment in jet engines we introduce the deadzone in the adaptation law and present simulations that successfully stabilize the system in the presence of noise and severe actuator saturation.

Keywords: Adaptive control; Jet engines; Time delay

1. Introduction

We consider the problem of stabilization of a class of MIMO LTI systems arising in models of various instabilities in jet engines. These instabilities often manifest themselves as oscillations, contaminated by noise. They are often caused by coupling of several resonant modes (structural, acoustic, of vortical) with time delays present in the physical process that couple the resonant modes. Often the control input is also subject to delay. Possible applications of the results in the paper include control of compressor blade flutter, rotating stall, and aeroacoustic instabilities (coupling of acoustic waves with vortex shedding from stator vanes).

Uncertain parameters abound in these problems: unknown or varying natural frequencies, uncertain delays due to poorly understood physical phenomena governing these processes, uncertain coupling between modes of oscillation, and of course, uncertain high frequency gains and delays of actuators. In this paper, we approach a class of such models using the tools of adaptive control.

Adaptive control of multivariable systems has received much less attention in the research community than the classical problems of adaptive control for SISO systems. The state of the art in model reference adaptive control for minimum phase systems is the paper by Ling and Tao (1997) where an adaptive backstepping technique was developed for MIMO LTI systems. Unfortunately, many of the models mentioned above are either not minimum phase, or possess delays that prevent applicability of a backstepping technique even when the delay is approximated by the Pade approximation. In such cases one needs to use a pole placement approach to adaptive control, which is well represented in the paper by Elliott, Wolovich, and Das (1984). This paper develops a direct adaptive technique. Unfortunately, direct adaptation, where the controller (instead of the plant) is parametrized, leads to heavy overparametrization of the problem, which is prohibitive in practice, where every redundant parameter estimate

☆This work was supported in part by grants F49620-01-C-0021 and FA9550-04-C-00442 from AFOSR.
*Corresponding author. Tel.: +1 858 822 1374; fax: +1 858 822 3107.
E-mail addresses: krstic@ucsd.edu (M. Krstic), banasza@utrc.utc.com (A. Banaszuk).
URL: http://mae.ucsd.edu/research/krstic/.

0967-0661/$ - see front matter © 2005 Elsevier Ltd. All rights reserved.
doi:10.1016/j.conengprac.2005.04.006

opens the door to nonrobustness to noise and unmodeled dynamics. An indirect adaptive scheme for MIMO systems, not only LTI but also LTV, was studied in the paper by Limanond and Tsakalis (2001). Our design in this paper is based on this general technique.

In physical models of instability of jet engines only a few specific physical parameters are uncertain. While the models may be of high order (say, tenth order, after the delay/s have been appropriately approximated, meaning the number of uncertain coefficients in the model is on the order of 20), the number of actual physical parameters that are uncertain will typically be 3–5 (those mentioned above). The transfer function coefficients will be nonlinear (typically multilinear or polynomial) functions of physical parameters. Nonlinear parametrizations do not lend themselves to parameter estimation. One typically has to overparametrize, i.e., define the products or powers of physical parameters as new parameters. Methods for avoiding this have been studied in Dasgupta (1988) and Sun (1993) and the references therein. However, these methods primarily succeed in improving accuracy of the estimates, and not in reducing the dynamic order of the parameter estimator to the minimum, i.e., to the number of actual uncertain physical parameters. To deal with this problem in the model considered here we develop an estimator based on the nonlinear parametrization. Our estimation error (also sometimes referred to as the "prediction error") has both linear and higher order dependence on the parameter estimation error, and is valid only locally. While this prevents us from proving any global results, it works exceptionally well in our application.

The paper is organized as follows. We start with the introduction of the model in Section 2. In Section 3 we make approximations to the delay terms that allow us to estimate the unknown delay and apply adaptive control. In Section 4 we introduce a frequency domain MIMO pole placement controller, which implicitly incorporates a reduced order observer, and present calculations that allow on-line determination of the pole-placement control gains based on the estimation of physical parameters. Section 5 introduces the filters and the update law for parameter estimation, and briefly argues local stability. Section 6 is dedicated to dealing with the effects of noise on the adaptive feedback scheme and the use of a deadzone to prevent parameter drift and bursting. In Section 7 we apply the adaptive controller in simulations to a model with a severe magnitude limit on control.

2. The model

Consider the model of the form

$$\ddot{y}_1 + \xi_{11}\dot{y}_1 + \eta_{11}y_1 + \zeta_{11}y_1(t-\tau_{11}) + \zeta_{12}y_2(t-\tau_{12}) = g_{11}\dot{u}_2(t-\tau_{c,1}) + h_{11}\chi_1, \quad (1)$$

$$\ddot{y}_2 + \xi_{22}\dot{y}_2 + \eta_{22}y_2 + \zeta_{22}y_2(t-\tau_{22}) + \zeta_{21}y_1(t-\tau_{21}) = g_{22}\dot{u}_1(t-\tau_{c,2}) + h_{22}\chi_2, \quad (2)$$

where y_1 and y_2 are temporal coefficients of the resonant modes, χ_1 and χ_2 are the disturbance inputs, and the parameters $\xi_{ij}, \eta_{ij}, \zeta_{ij}, \tau_{ij}, g_{ij}, h_{ij}, \tau_{c,i}$ are uncertain. Such a model is common in case where two resonant modes with close resonant frequencies couple though a physical process that involves transport delays.

To motivate this model and the adaptive control problem considered in this paper, we use a simplified version of a model for control of thermoacoustic instabilities on annular domain (Banaszuk, Hagen, Mehta, & Oppelstrup, 2003).

Thermoacoustic instabilities in gas turbine and rocket engines develop when acoustic waves in combustors couple with an unsteady heat release field in a positive feedback loop. They manifest themselves as high amplitude pressure oscillations close to resonant acoustic frequencies of the combustor. The oscillations can lead to structural damage of the combustor and cannot be tolerated. Control of thermoacoustic instabilities using high speed fuel valves and pressure sensors was demonstrated in numerous experiments in academia and industry (Candel, 1992). Including a demonstration on a full scale industrial gas turbine (Seume et al., 1997). A simple phase-shifting controller with an appropriately chosen phase-shift was typically sufficient for suppression of oscillations, given enough control authority, but the control phase and gain had to be adjusted manually, at every operating condition. The difficulty in determining the optimal phase shift that minimizes pressure oscillations, either by analysis or by experiment, especially in large industrial-scale combustors that operate over a wide range of conditions, has led researchers to call for the use of adaptive schemes (Seume et al., 1997). A direct adaptive scheme (based on extremum-seeking) applicable to control of thermoacoustic modes with large separation in frequencies (and hence essentially decoupled) was recently demonstrated in a 4 MW industrial rig in Banaszuk, Ariyur, Krstic, and Jacobson (2004). Benefits and limitations of the extremum seeking scheme were examined in Ariyur and Krstic (2003). In this paper, we investigate an indirect adaptive scheme that overcomes some of the limitations of the direct scheme and is applicable to the case of multiple acoustic modes with close or identical frequencies (so that the decoupling assumption is not applicable).

We consider an annular combustor that includes a circumferential array of bluff body flame holders. Flameholders extend radially from inner to outer diameter of the annular combustor. A cut along a constant radius surface is shown in Fig. 1.

For the purpose of modeling, we assume that the fuel mass fraction defined at the fuel injection surface $x_0(y,z)$

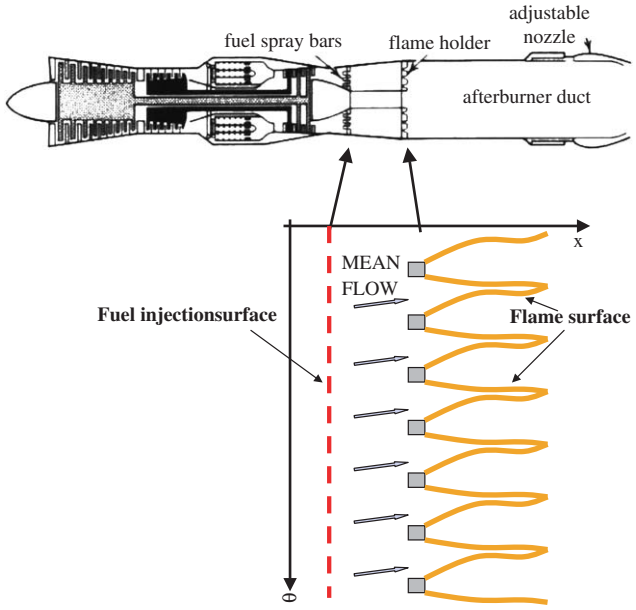

Fig. 1. 2D cut at a constant radius across the combustor showing a bluff body flameholder array, fuel injection surface upstream of flameholders, and flame surface downstream of flameholders.

is advected downstream to the fixed but distributed flame surface $x = g_{fl}(y,z)$ by the sum of the mean and acoustic perturbation velocity (without diffusion). The mean fuel mass fraction at the fuel injection surface is $\overline{Y}_f(x_0,y,z) = \overline{\chi}_f(x_0,y,z)/\overline{\chi}_a(x_0,y,z)$, where $\chi_f = \rho_f U_f$, $\chi_a = \rho_a U_a$ denote the flux and ρ_f, ρ_a are the fuel and air densities and U_f, U_a are the velocities. We define relative perturbations of pressure and heat release as $\tilde{p}(x,y,z,t) := p'(x,y,z,t)/\gamma\overline{p}(x,y,z)$ and $\tilde{q}(x,y,z,t) := (\gamma-1)/\gamma\, q'(x,y,z,t)/\overline{p}(x,y,z)$, where γ is the ratio of specific heats. Using the isentropic assumption we can express density perturbation as a function of pressure perturbation as

$$\frac{\rho_a'}{\overline{\rho}_a} = \frac{1}{\gamma}\frac{p'}{\overline{p}} = \tilde{p}. \tag{3}$$

Assuming the air velocity perturbation due to acoustics is negligible relative to the density perturbation we can now express the perturbation fuel mass fraction (in the presence of acoustics) as

$$\begin{aligned} &y_f(x_0,y,z,t) \\ &\quad = \overline{Y}_f(x_0,y,z)\left(\frac{\chi_f'(x_0,y,z,t)}{\overline{\chi}_f(x_0,y,z)} - \frac{\chi_a'(x_0,y,z,t)}{\overline{\chi}_a(x_0,y,z)}\right) \\ &\quad = \overline{Y}_f(x_0,y,z)\left(\frac{u_f'(x_0,y,z,t)}{\overline{u}_f(x_0,y,z)} - \tilde{p}(x_0,y,z,t)\right), \end{aligned} \tag{4}$$

where the fuel velocity $u_f'(x_0,y,z,t)$ is the control variable. The first term on the right-hand side of (4) represents the effect of fuel control action and the second term represents the effect of acoustic velocity perturbation.

The fuel–air mixture convects to the fixed flame surface $x = g_{fl}(y,z)$ and the heat release density at the flame surface is obtained as

$$Q(x,y,z,t) = F_{hr}(Y_f(x,y,z,t))\gamma_{flame}(x - g_{fl}(y,z)), \tag{5}$$

where $\gamma_{flame}(\cdot)$ is the axial heat release distribution function representing the flame thickness, and $F_{hr}(\cdot)$ describes local heat release as function of local fuel mass fraction.

We also assume that the acoustic velocity perturbation is purely potential, i.e., $\mathbf{u}'(x,y,z,t) = \nabla\phi(x,y,z,t)$ for some smooth scalar $\phi(x,y,z,t)$ called the *velocity potential*. Under additional assumption that the mean fuel mass fraction is uniform downstream of flameholders, we obtain a linear distributed thermoacoustic model (see Banaszuk et al., 2003 for details) as

$$\begin{aligned} &\frac{\partial}{\partial t}\tilde{p}(x,y,z,t) + \overline{\mathbf{u}}(x,y,z)\cdot\nabla\tilde{p}(x,y,z,t) + \Delta\phi(x,y,z,t) \\ &\quad = \tilde{q}(x,y,z,t), \end{aligned} \tag{6}$$

$$\begin{aligned} &\frac{\partial}{\partial t}\phi(x,y,z,t) + \overline{\mathbf{u}}(x,y,z)\cdot\nabla\phi(x,y,z,t) + a^2\tilde{p}(x,y,z,t) \\ &\quad = \eta(x,y,z,t), \end{aligned} \tag{7}$$

$$\frac{\partial}{\partial t}y_f(x,y,z,t) + \overline{\mathbf{u}}(x,y,z)\cdot\nabla y_f(x,y,z,t) \quad = 0, \tag{8}$$

$$\begin{aligned} &\tilde{q}(x,y,z,t) \\ &\quad = F_{hr}'(\overline{Y}_f(x,y,z))\gamma_{flame}(x - g_{fl}(y,z))y_f(x,y,z,t), \end{aligned} \tag{9}$$

where driving disturbance (broad-band noise) $\eta(x,y,z,t)$ represents the effect of local turbulence.

The acoustic boundary conditions are provided on the combustor boundary surface in terms of the normal velocity $\mathbf{u}_n'(\mathbf{x},t) = \nabla\phi(\mathbf{x},t)\cdot\hat{n}(\mathbf{x})$ (where $\hat{n}(\mathbf{x})$ is the normal vector to the boundary). The acoustic boundary condition serves as another possible control input. We assume that the acoustic boundary conditions are described by a local admittance relation (described here in the frequency domain)

$$U_n'(\mathbf{x},j\omega) = G^{bc}(\mathbf{x},j\omega)\tilde{P}(\mathbf{x},j\omega) \tag{10}$$

(see e.g. Morse & Ingard, 1968) for $\mathbf{x}\in\mathscr{S}$, where $\mathscr{S}$ denotes the boundary surface.

The fuel–air mixture is responsible for the burning at the flame and the subsequent heat release. This heat release at the flame surface excites the acoustic waves in the combustor volume. The acoustic waves in turn travel upstream and perturb the transport of the fuel/air mixture. This feedback coupling can lead to instability if the driving resulting from this feedback mechanism dominates the damping resulting from absorption of the acoustic energy at the boundary. Control over fuel rate at the fuel injection surface $x_0(y,z)$, control of the shear

layer dynamics using flow control at the flameholders, or control of the air injection at the combustor boundary can provide ways of influencing the process and eliminating instability. The control could be provided at various temporal and spatial scales.

Now we introduce a reduced order model suitable for control design obtained from the thermoacoustic instability model presented above. The model is also suitable for optimization of the control architecture. In order to obtain model reduction, we expand the pressure and potential perturbations in terms of the acoustic modes $\{\Pi_k(\mathbf{x})\}_{k=1,2,\ldots}$ as $\tilde{p}(\mathbf{x},t)=\sum_k y_k(t)\Pi_k(\mathbf{x})$, $\phi(\mathbf{x},t)=\sum_k \phi_k(t)\Pi_k(\mathbf{x})$ and apply standard Galerkin procedure involving integration by parts and using the admittance condition (10) (see Banaszuk et al., 2003 for details) to obtain a two-mode model represented in the frequency domain as

$$j\omega\begin{bmatrix}\Phi_1(j\omega)\\ \Phi_2(j\omega)\\ Y_1(j\omega)\\ Y_2(j\omega)\end{bmatrix}=\begin{bmatrix}0&0&-a^2&0\\ 0&0&0&-a^2\\ \lambda_1&0&0&0\\ 0&\lambda_2&0&0\end{bmatrix}\begin{bmatrix}\Phi_1(j\omega)\\ \Phi_2(j\omega)\\ Y_1(j\omega)\\ Y_2(j\omega)\end{bmatrix}+\begin{bmatrix}N_1(j\omega)\\ N_2(j\omega)\\ Q_1(j\omega)-V_1(j\omega)\\ Q_2(j\omega)-V_2(j\omega)\end{bmatrix},\tag{11}$$

where $Y_m(j\omega)$ is the Fourier transform of $y_m(t)$, $\Phi_m(j\omega)$ is the Fourier transform of $\phi_m(t)$, and $Q_m(j\omega)$, $N_m(j\omega)$, and $V_m(j\omega)$ denote the Fourier transforms of

$$q_m(t)=\int_{\mathscr{V}}\Pi_m(\mathbf{x})\tilde{\mathbf{q}}(\mathbf{x},\mathbf{t})\,\mathrm{d}\mathbf{x},\tag{12}$$

$$\eta_m(t)=\int_{\mathscr{V}}\Pi_m(\mathbf{x})\tilde{\eta}(\mathbf{x},\mathbf{t})\,\mathrm{d}\mathbf{x},\tag{13}$$

$$v_m(t)=\int_{\mathscr{S}}\Pi_m(\mathbf{x})\mathbf{u}'_{\mathbf{n}}(\mathbf{x},\mathbf{t})\,\mathrm{d}\mathbf{x},\tag{14}$$

respectively, and $\lambda_m:=\int_{\mathscr{V}}|\nabla\Pi_m(\mathbf{x})|^2\,\mathrm{d}\mathbf{x}/\int_{\mathscr{V}}|\Pi_m(\mathbf{x})|^2\,\mathrm{d}\mathbf{x}$ ($\mathscr{V}$ and $\mathscr{S}$ denotes the combustor volume and boundary surface, respectively). Solving (11) for the velocity potential coefficient as function of pressure and perturbation coefficients yields the formula

$$\Phi_1(j\omega)=\frac{-a^2}{j\omega}\,Y_k(j\omega)+\frac{1}{j\omega}N_k(j\omega),\quad k=1,2.\tag{15}$$

Now we can simplify (11) as follows:

$$((j\omega)^2+\lambda_k a^2)Y_k(j\omega)=(j\omega)(Q_k(j\omega)-V_k(j\omega))+\lambda_k N_k(j\omega),\quad k=1,2.\tag{16}$$

The fuel velocity $u'_f(x_0(y,z),y,z,t)$ at the fuel injection surface is the control variable. We assume that the control is realized using N_{inj} fuel injectors with ith fuel injector providing fuel mass flux equal $w_{f,i}(t)$ with spatial distribution $k_{f,i}(y,z)$ (representing initial fuel spread in the direction perpendicular to the mean flow). Thus, we will represent the distributed velocity as $u'_f(x_0(y,z),y,z,t)=\sum_{i=1}^{N_{inj}}k_{f,i}(y,z)w_{f,i}(t)$, with $w_{f,i}(t)$ representing the control inputs. Since we will be interested in controlling two acoustic modes, we will further assume the control in the frequency domain as

$$W_{f,k}(j\omega)=\sum_i \Gamma_{ki}Z_i(j\omega).\tag{17}$$

The quantities $Z_k(j\omega)$ will be the new control inputs. The coefficients Γ_{ki} will be determined later to simplify the control design.

Let us assume that we are dealing with a reduced order model describing evolution of two acoustic eigenmodes corresponding to a double imaginary eigenvalue and assume that the acoustic mode Π_2 is obtained from the acoustic mode Π_1 by rotation by 90°. In this case, because of rotational symmetry of the annular domain, one can verify that $G_{11}^{\phi 2q}=G_{22}^{\phi 2q}$, $G_{21}^{\phi 2q}=-G_{12}^{\phi 2q}$, etc. Let

$$G^z_{mk}(j\omega):=\sum_{i=1}^{N_{inj}}G_{mi}^{u_f 2q}(j\omega)\Gamma_{ki}.\tag{18}$$

The closure equations to (11) are given by

$$V_m(j\omega)=G_m^{bc}(j\omega)\,Y_m(j\omega),\tag{19}$$

$$Q_m(j\omega)=\sum_{k=1}^{2}G_{mk}^{p2q}(j\omega)\,Y_m(j\omega)+\sum_{i=1}^{N_{inj}}G_{mi}^{u_f 2q}(j\omega)W_{f,i}(j\omega).\tag{20}$$

The transfer functions in the above expression have the form

$$G_m^{bc}(j\omega):=\int_{\mathscr{S}}G^{bc}(\mathbf{x},j\omega)|\Pi_m(\mathbf{x})|^2\,\mathrm{d}\mathbf{x},\tag{21}$$

$$G_{mk}^{p2q}(j\omega)=\int_{\mathscr{W}}k_{mk}^{p2q}(y,z)\mathrm{e}^{-j\omega\tau(y,z)}\,\mathrm{d}y\,\mathrm{d}z,\tag{22}$$

$$G_{mi}^{u_f 2q}(j\omega)=\int_{x_0}k_{mi}^{u_f 2q}(y,z)\mathrm{e}^{-j\omega\tau(y,z)}\,\mathrm{d}y\,\mathrm{d}z,\tag{23}$$

$$k_{mk}^{p2q}(y,z):=-\Pi_k(x_0(y,z),y,z)\Pi_m(g_{fl}(y,z),y,z)\times F'(\overline{Y}_f(y,z)),\tag{24}$$

$$\tau(y,z):=\frac{g_{fl}(y,z)-x_0(y,z)}{\overline{u}(y,z)},\tag{25}$$

$$k_{mi}^{u_f 2q}(y,z):=\frac{k_{f,i}(y,z)}{\overline{u}_f(x_0(y,z),y,z)}\,\Pi_m(g_{fl}(y,z),y,z)\times F'(\overline{Y}_f(y,z)).\tag{26}$$

Now, combining Eqs. (16), (20), and (20), we obtain

$$((j\omega)^2 + (j\omega)G_k^{bc}(j\omega) + \lambda_k a^2)Y_k(j\omega) = \sum_{m=1}^{2}(j\omega)G_{km}^{p2q}Y_m(j\omega) + \sum_{i=1}^{N_{inj}} G_{mi}^{u_f 2q}(j\omega)(j\omega)W_{f,i}(j\omega) + \lambda_k N_k(j\omega), \quad k = 1, 2. \tag{27}$$

While the reduced order frequency domain model looks simple, it is in fact an infinite dimensional model, as the heat release response transfer functions include a distributed delay. Moreover, the parameters describing the model (mean flow, flame, fuel distribution, boundary condition admittance) are known only approximately, and hence need to be estimated. The distributed delay model parameter estimation is not tractable. We will simplify the model further, replacing the distributed delays by (unknown) lumped delays. This is a reasonable approximation in a narrow frequency band around the acoustic mode resonant frequency.

The first simplifying assumption is that the acoustic boundary admittance (20) is a real positive number, that is

$$G_k^{bc}(j\omega) = \xi_{kk}. \tag{28}$$

This is a reasonable assumption since in the engines the acoustic boundary conditions are designed to maximize the real and minimize the imaginary part of the admittance for optimal acoustic damping.

The second simplifying assumption is that the heat release transfer functions representing the distributed delay can be represented as (20) is a real positive number, that is

$$G_{kk}^{u_f 2q}(j\omega) \approx g_{kk}\, \mathrm{e}^{j\omega\tau_{c,k}}, \tag{29}$$

$$(j\omega)G_{km}^{p2q}(j\omega) \approx -\zeta_{km}\, \mathrm{e}^{j\omega\tau_{km}}, \tag{30}$$

for some ζ_{km}, τ_{km}, $k, m = 1, 2$. These assumptions are justified by the fact that in the narrow frequency band around the acoustic resonant frequency $\omega_k := a\sqrt{\lambda_k}$ any transfer function with relatively flat magnitude response and rolling off phase response can be approximated as a lumped delay and a static gain. Now, Eq. (27), when represented in time domain, becomes (1) (with $h_{kk} = \lambda_k$).

In this paper, we are interested in a particular case of (1) when, because of the assumption of circular symmetry of the combustor, (1) models the strong cross-coupling of identical lightly damped resonant modes represented by the equations

$$\ddot{y}_1 + \eta y_1 + \zeta y_2(t-\tau) = g\dot{u}_2(t-\tau) + h\chi_1, \tag{31}$$

$$\ddot{y}_2 + \eta y_2 - \zeta y_1(t-\tau) = -g\dot{u}_1(t-\tau) + h\chi_2. \tag{32}$$

We assume that pressure measurements $\tilde{p}(\mathbf{x}_i, t) = \sum_{k=1}^{2} y_k(t)\Pi_k(\mathbf{x}_i)$ at at least two locations $\mathbf{x}_i$ are available. This allows to reconstruct the model coefficients $y_k(t)$. Therefore, we will assume that the coefficients $y_k(t)$ are directly available for measurement. We also assume that disturbance terms $N_1(j\omega)$, $N_2(j\omega)$ are broad band uncorrelated stochastic processes. The objective of the feedback control is to reduce the pressure terms P_1, P_2 to guarantee that the pressure level is below acceptable level.

3. Approximating the delay

We denote $f = 2/\tau$, take the Laplace transform of (31), (32), and get a control model:

$$((s^2 + \eta)I + \zeta P\, \mathrm{e}^{-2s/f})y = g\, \mathrm{e}^{-2s/f} sPu + h\chi, \tag{33}$$

where

$$y = [y_1 \quad y_2]^{\mathrm{T}}, \tag{34}$$

$$u = [u_1 \quad u_2]^{\mathrm{T}} \tag{35}$$

and I is a 2×2 identity matrix, whereas P is defined as

$$P = \begin{bmatrix} 0 & 1 \\ -1 & 0 \end{bmatrix}. \tag{36}$$

To model the delay, we use the first-order Pade approximation. A second-order Pade would be more appropriate to *simulate* a delay, but for *control design*, especially adaptive, where inaccuracy in the order of approximation at relevant frequencies can be accommodated by automatic adjustment of the delay parameter estimate to produce the right phase, first-order Pade should be sufficient. Moreover, higher order Pade would complicate the parametrization issues for adaptive control. Thus,

$$\mathrm{e}^{-2s/f} \approx \frac{f - s}{f + s}. \tag{37}$$

With this approximation, we can write the model in one of the standard forms for MIMO systems:

$$A(s)y = B(s)u + C(s)\chi, \tag{38}$$

where

$$A(s) = Is^3 + fIs^2 + Q^{\mathrm{T}}s + fQ, \tag{39}$$

$$B(s) = g(f - s)sP, \tag{40}$$

$$C(s) = h(s + f)I \tag{41}$$

and

$$Q = \eta I + \zeta P. \tag{42}$$

Even though the model "denominator" is third-order, since the coefficients are 2×2 matrices, the model is of order 6.

4. Frequency domain pole placement MIMO design

We will use a compensator of the form

$$(Is^2 + D_1 s + D_0)u = -(N_2 s^2 + N_1 s + N_0)y. \tag{43}$$

This structure is capable of the same type of pole placement + Luenberger observer design as the state space methods. The fact that the compensator order is lower by 2 (or 1 in the matrix sense) than the plant is due to this structure using a reduced order observer.

The coefficients in the above compensator are matrices which need to be computed by solving a polynomial (Bezout) equation with matrix coefficients to place the closed-loop poles at the location of the polynomial (again with matrix coefficients)

$$\alpha(s) = (s^5 + \alpha_4 s^4 + \alpha_3 s^3 + \alpha_2 s^2 + \alpha_1 s + \alpha_0)I. \tag{44}$$

Note that, while the α_i's are scalars, I is multiplying the whole polynomial. This polynomial will be the matrix denominator of the entire closed-loop system. The closed loop system will be or order 10, where 6 integrators come from the plant and 4 come from the compensator.

The pole placement approach is uniquely suited for the given plant. The plant is not minimum phase, even for $f = \infty$, i.e., without delay (by inspection of $y = A(s)^{-1}B(s)u$ one can see that, in addition to a zero at the origin, there is a pair of zeros on the imaginary axis). The presence of any Pade approximation of the delay makes the system strictly non-minimum phase. Since the control objective is stabilization, not tracking, pole placement (where one does not pursue assignment of closed-loop zeros, which cannot be done stably for a nonminimum phase system) is an appropriate approach, which is also compatible with adaptation. One cannot pursue adaptive model reference control, which requires a minimum phase plant.

The solution of the Bezout equation

$$D(s)A(s) + B(s)N(s) = \alpha(s) \tag{45}$$

for the compensator coefficient matrices is

$$D_0 = \frac{\alpha_0}{f(\eta^2 + \zeta^2)} Q^{\mathrm{T}}, \tag{46}$$

$$D_1 = \frac{1}{2f(\eta + f^2)}(\bar{\alpha}_1 I - D_0(2f^2 I + Q^{\mathrm{T}})), \tag{47}$$

$$N_0 = \frac{1}{g} P^{\mathrm{T}}(D_1(2f^2 I + Q^T) + 2fD_0 - \bar{\alpha}_2 I), \tag{48}$$

$$N_1 = \frac{1}{g} P^{\mathrm{T}}(2fD_1 + D_0 + Q^{\mathrm{T}} - \bar{\alpha}_3 I), \tag{49}$$

$$N_2 = \frac{1}{g} P^{\mathrm{T}}(D_1 - \bar{\alpha}_4 I), \tag{50}$$

where

$$\bar{\alpha}_4 = \alpha_4 - f, \tag{51}$$

$$\bar{\alpha}_3 = \alpha_3 + f\bar{\alpha}_4, \tag{52}$$

$$\bar{\alpha}_2 = \alpha_2 + f\bar{\alpha}_3 - 2f\eta, \tag{53}$$

$$\bar{\alpha}_1 = \alpha_1 + f\bar{\alpha}_2. \tag{54}$$

Note the recursive character of these relations, and that the right order to compute the quantities is $\bar{\alpha}_4 \to \bar{\alpha}_3 \to \bar{\alpha}_2 \to \bar{\alpha}_1 \to D_0 \to D_1 \to N_0 \to N_1 \to N_2$.

The plant parameters η, ζ, g, f are unknown and will be estimated on-line. Their estimates are denoted by $\hat{\eta}, \hat{\zeta}, \hat{g}, \hat{f}$. To obtain the estimates $\hat{D}_i, \hat{N}_i$ of the controller parameter matrices D_i, N_i, replace η, ζ, g, f by $\hat{\eta}, \hat{\zeta}, \hat{g}, \hat{f}$ and $Q = \eta I + \zeta P$ by

$$\hat{Q} = \hat{\eta} I + \hat{\zeta} P \tag{55}$$

in (46)–(54). The state space (implementation-ready) representation of the pole placement compensator (43) is

$$\dot{\lambda} = \begin{bmatrix} -\hat{D}_1 & I \\ -\hat{D}_0 & 0 \end{bmatrix} \lambda + \begin{bmatrix} \hat{D}_1 \hat{N}_2 - \hat{N}_1 \\ \hat{D}_0 \hat{N}_2 - \hat{N}_0 \end{bmatrix} y, \tag{56}$$

$$u = [I \quad 0]\lambda - \hat{N}_2 y. \tag{57}$$

Note that this system is of order 4.

5. Adaptation law

Because the plant, even though high dimensional and MIMO, includes only a few uncertain physical parameters, η, ζ, g, f, it is amenable to the use of "indirect" adaptive control, which employs an estimator of a small number of plant parameters, rather than an estimator of a high number of controller parameters. To make this statement quantitative, we will be estimating only 4 parameters, whereas a "direct" adaptive scheme for a plant of this structure would estimate up to 20 parameters.

From (38)–(42), setting $\chi = 0$, we get the parametric model

$$\frac{\mathrm{d}^3}{\mathrm{d}t^3} y_1 + f\ddot{y}_1 + \eta\dot{y}_1 - \zeta\dot{y}_2 + f\eta y_1 + f\zeta y_2 + g\ddot{u}_2 - fg\dot{u}_2 = 0. \tag{58}$$

This parametric model is linear but involves three derivatives, which are not available for implementation. The standard tool is to employs third-order filters,

$$\dot{\phi}_1 = \phi_2, \tag{59}$$

$$\dot{\phi}_2 = \phi_3, \tag{60}$$

$$\dot{\phi}_3 = -l_0\phi_1 - 1\phi_2 - l_2\phi_3 + y_1, \tag{61}$$

$$\dot{\psi}_1 = \psi_2, \tag{62}$$

$$\dot{\psi}_2 = \psi_3, \tag{63}$$

$$\dot{\psi}_3 = -l_0\psi_1 - 1\psi_2 - l_2\psi_3 + y_2, \tag{64}$$

$$\dot{\omega}_1 = \omega_2, \tag{65}$$

$$\dot{\omega}_2 = \omega_3, \tag{66}$$

$$\dot{\omega}_3 = -l_0\omega_1 - 1\omega_2 - l_2\omega_3 + u_2, \tag{67}$$

where $l(s) = s^3 + l_2s^2 + l_1s + l_0$ should be chosen Hurwitz. Assuming zero initial conditions, we get

$$y_1 - l_2\phi_3 - l_2\phi_2 - l_0\phi_1 + \eta\phi_2 - \zeta\psi_2 + g\omega_3 + f(\phi_3 + \eta\phi_1 + \zeta\psi_1 - g\omega_2) = 0. \tag{68}$$

Let us now denote the vector of unknown parameters and the vector of their estimates, respectively as

$$\theta = \begin{bmatrix} \eta \\ \zeta \\ g \\ f \end{bmatrix}, \quad \hat{\theta} = \begin{bmatrix} \hat{\eta} \\ \hat{\zeta} \\ \hat{g} \\ \hat{f} \end{bmatrix}. \tag{69}$$

A straightforward but relatively lengthy calculation leads to

$$\begin{aligned} y_1 - l_2\phi_3 - l_2\phi_2 - l_0\phi_1 + \hat{\eta}\phi_2 - \hat{\zeta}\psi_2 + \hat{g}\omega_3 \\ + \hat{f}(\phi_3 + \hat{\eta}\phi_1 + \hat{\zeta}\psi_1 - \hat{g}\omega_2) \\ = -\Omega^{\mathrm{T}}\tilde{\theta} + \tilde{\theta}^{\mathrm{T}}\Sigma\tilde{\theta}, \end{aligned} \tag{70}$$

where $\tilde{\theta} = \theta - \hat{\theta}$ (and similarly for η, ζ, g, f), the "regressor" vector is defined as

$$\Omega = \begin{bmatrix} \phi_2 + \hat{f}\phi_1 \\ -\psi_2 + \hat{f}\psi_1 \\ \omega_3 - \hat{f}\omega_2 \\ \phi_3 + \hat{\eta}\phi_1 + \hat{\zeta}\psi_1 - \hat{g}\omega_2 \end{bmatrix} \tag{71}$$

and "second-order" effects (of the parameter error $\tilde{\theta}$) are given by the matrix

$$\Sigma = \begin{bmatrix} 0 & 0 & 0 & 0 \\ 0 & 0 & 0 & 0 \\ 0 & 0 & 0 & 0 \\ -\phi_1 & -\psi_1 & \omega_2 & 0 \end{bmatrix}. \tag{72}$$

We now choose the update law for the pole placement algorithm as

$$\begin{aligned} \dot{\hat{\theta}} = -\Gamma\frac{\Omega}{1+\gamma|\Omega|^2}(y_1 - l_2\phi_3 - l_1\phi_2 - l_0\phi_1 + \hat{\eta}\phi_2 - \hat{\zeta}\psi_2 \\ + \hat{g}\omega_3 + \hat{f}(\phi_3 + \hat{\eta}\phi_1 + \hat{\zeta}\psi_1 - \hat{g}\omega_2)), \end{aligned} \tag{73}$$

where γ is a positive constant and Γ is a positive definite symmetric matrix that can either be constant (in which case the update law is of the gradient type) or be computed via a Riccati equation

$$\dot{\Gamma} = -\Gamma\frac{\Omega\Omega^{\mathrm{T}}}{1+\gamma|\Omega|^2}\Gamma \tag{74}$$

which makes the update law of the least-squares type. The stability of the update law (73) can be studied by writing it as

$$\dot{\tilde{\theta}} = -\Gamma\frac{\Omega\Omega^{\mathrm{T}}}{1+\gamma|\Omega|^2}\tilde{\theta} + \Gamma\frac{\Omega}{1+\gamma|\Omega|^2}\tilde{\theta}^{\mathrm{T}}\Sigma\tilde{\theta}, \tag{75}$$

where we note the stabilizing effect of the first term on the right-hand side (linear in $\tilde{\theta}$) and the potentially destabilizing effect of the second term (quadratic in $\tilde{\theta}$). We refrain from stating theorems and proofs in this paper. However, it is possible to establish local stability of the parameter error system (75) under an appropriate persistency of excitation condition. It is also possible to establish local closed-loop stability of the overall system consisting of the plant, the adaptive pole placement controller, and the filters, and the update law.

Due to the presence of the quadratic term, the estimator (73) is only locally stable. A globally stable estimator for the parametric model (68) would require $f\eta, f\zeta, fg$ to be estimated separately from η, ζ, g, f, i.e., it would require *overparametrization*. Overparametrization not only increases the dynamic order of the compensator (by 3 in the case of gradient adaptation, and by as much as 36 in the case of least-squares adaptation), but it aggravates the robustness issues because the persistency of excitation conditions are much harder to satisfy for 7 parameters than for 4 parameters.

The block diagram of the closed-loop adaptive system is shown in Fig. 2. The adaptive controller consists of three major blocks: the adaptive pole placement compensator (which includes the state λ and the on-line adjusted $\hat{N}_i$'s and $\hat{D}_i$'s), the parameter estimator (consisting of filters ϕ, ψ, ω, the computation of the regressor, the estimation error, and the update law), and the Bezout solver (which computes the $\hat{N}_i$'s and $\hat{D}_i$'s on the basis of $\hat{\theta}$). The dynamic order of the parameter estimator is 13 (for the gradient update): 9 for the filter states ϕ, ψ, ω, and 4 for the parameter estimate $\hat{\theta}$. The total dynamic order of the adaptive controller (including the λ states) is 17.

6. Dealing with the noise

It is important to first understand the noise rejection properties of the nonadaptive system, designed with the perfect knowledge of the parameters. Combining (45) with (38), one gets

$$y = S(s)\chi, \tag{76}$$

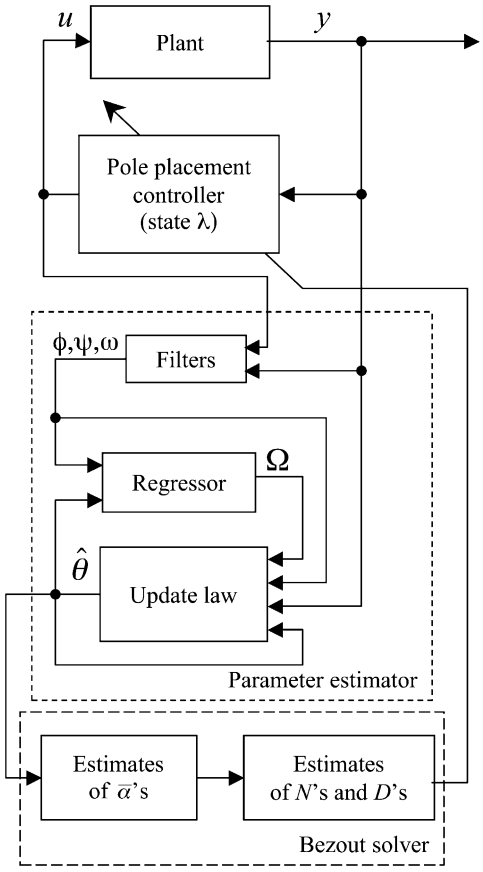

Fig. 2. Adaptive system block diagram.

where

$$S(s) = \frac{h(s+f)}{s^5 + \alpha_4 s^4 + \alpha_3 s^3 + \alpha_2 s^2 + \alpha_1 s + \alpha_0}\,(Is^2 + D_1 s + D_0). \tag{77}$$

Note that D_0 and D_1 depend on the α_i's [through (46)–(54)] and on η, ζ, g, f. One can influence the H_∞ norm of the sensitivity function $S(s)$ by varying the α_i's. Assuming that one has persistency of excitation, the α_i's also become a tool for noise rejection in the adaptive case because the estimates of η, ζ, g, f would converge to the true values.

The biggest issue in the adaptive case is that the noise can cause the parameter estimates to drift. The scenario is usually as follows. The unstable plant generates enough percistency of excitation for the parameter estimates to enter the region of stabilizing values in the parameter space. This "stabilizes" the plant state to a small value. However, then the noise, whose value was small to make a difference relative to the unstable transient of the open-loop system, takes over. The adaptation starts being dominated by the noise. The parameter estimates start to "drift". After sufficient time, they drift out of the region of stabilizing parameter values. The moment they exit this region, the system output starts growing. This, in turn, generates persistency of excitation, where the signals are again dominated by the plant transient, rather than the noise. The excitation returns the estimates to the stabilizing region in the parameter space. This entire process of the parameters being returned to the stabilizing region is fast and is referred to as a "burst." Bursting is undesirable because the size of the output regains the values comparable to those during the initial learning transient. Bursting is periodic in appearance and continues as long as the adaptation is active. The good asymptotic performance, the very reason for employing adaptive control, is lost.

Fortunately, a solution to the problem of parameter drift and bursting does exist. It is the *deadzone* that is applied to the estimation error. The parameter update is modified as

$$\dot{\hat{\theta}} = -\Gamma \frac{\Omega}{1+\gamma|\Omega|^2}\, \Delta_b(y_1 - l_2\phi_3 - l_1\phi_2 - l_0\phi_1 + \hat{\eta}\phi_2 - \hat{\zeta}\psi_2 + \hat{g}\omega_3 + \hat{f}(\phi_3 + \hat{\eta}\phi_1 + \hat{\zeta}\psi_1 - \hat{g}\omega_2)), \tag{78}$$

where $\Delta_b(\cdot)$ represents the deadzone nonlinearity with a threshold (break point) b and with a slope equal to one outside of the deadzone. The deadzone prevents bursting by not adapting to small estimation errors, which would primarily be caused by the noise.

7. Simulations with saturated actuator

We present simulations done for the plant (38), employing the controller (56), the filters (59)–(67), the update law (78), and the algebraic equations (46)–(54). In addition, the control inputs u_1 and u_2 were saturated.

The plant was represented in the MIMO observer canonical form. For the simulations presented here the plant initial condition was $y_1(0) = 1, y_2(0) = 0$, and all the derivatives of the outputs set initially to zero. The design was also tested for a wide variety of initial conditions and has failed only for those choices unreasonably above the saturation level of the control inputs. The plant parameters were all set to unity, $\eta = \zeta = g = f = h = 1$. With these parameters the open-loop plant was unstable, with eigenvalues $-1.3 \pm j0.75, +0.11 \pm j1.4, +0.23 \pm j0.63$. One of the zeros was unstable, at $+1$.

The noise power was set to a fairly high value (for this problem) of 0.25. The control inputs were limited to the interval $[-3.5, 3.5]$.

The desired closed-loop poles were at $-2, -2, -2, -1.5 \pm j0.5$. By varying the desired poles one can improve the performance and robustness. We did not try to do this here. Rather than present results polished through extensive trial and error, we show that the design is successful even when the design parameter choices are made without much experience and insight.

Guided by the same logic, the initial conditions of the compensator and the filters were all chosen zero, $\lambda(0)=0, \phi(0)=\psi(0)=\omega(0)=0$. The filter poles were chosen at $-4, -3\pm j1.7$, which is faster than the desired closed-loop poles, indicating that we want the parameter estimation to complete fast. For adaptation parameters we have chosen $\Gamma = 10I$ and $\gamma = 1$.

The initial values for the estimates of the unknown parameters were chosen with a little more care:

- $\hat{\eta}(0)$: Among the four parameters, this one, being the natural frequency of the open-loop plant, is the one that is the least uncertain. We have chosen $\hat{\eta}(0) = 1.3\eta$.
- $\hat{g}(0)$: Since we have limited control authority, it is better to not start off too agressively with control. If we chose $\hat{g}(0)$ small, this would signal to the compensator that it needs to put out a large input because its gain is small. So we have chosen this parameter large, $\hat{g}(0) = 2g$.
- $\hat{f}(0)$: Since the delay introduces a non-minimum phase effect in the Pade approximated plant, it is important to not underestimate the value of the delay. Thus, we start with $\hat{f}(0)$ chosen large, $\hat{f}(0) = 2.4f$.
- $\hat{\zeta}(0)$: The parameter ζ is the measure of coupling between the two subsystems. By choosing $\hat{\zeta}(0)$ small, we would be deceiving ourselves that the coupling is small and we would start the control with a predominantly SISO design. Thus we start with $\hat{\zeta}(0)$ set to a relatively large value, $\hat{\zeta}(0) = 1.7\zeta$.

These initial estimates are actually destabilizing—without adaptation this controller would not work.

For selecting the deadzone breakpoint b we first ran the simulations without the deadzone. As predicted, the parameter estimates drifted and they, as well as the system output, went through periodic bursting. The value of the deadzone was chosen based on the value of noise driven estimation error, $y_1 - l_2\phi_3 - l_1\phi_2 - l_0\phi_1 + \hat{\eta}\phi_2 - \hat{\zeta}\psi_2 + \hat{g}\omega_3 + \hat{f}(\phi_3 + \hat{\eta}\phi_1 + \hat{\zeta}\psi_1 - \hat{g}\omega_2)$. It was set at $b = 0.06$. A much smaller value would still result in bursting. A much larger value would prevent adaptation, the estimates would stay at their initial values, and the system would go unstable.

Fig. 3 shows simulation results. We do not show both outputs y_1 and y_2, nor do we show both inputs, u_1 and u_2. They are qualitatively similar between each other. We show only the first output $y_1(t)$ and the second input $u_2(t)$.

The time traces show four distinct intervals in the behavior of the system:

- During the first interval, approximately up to 15 s, the system output is growing because the initial control parameters have destabilizing values. The adaptation is starting slow because the signals to drive it need to get large first.
- During the second interval, from 15 to 20 s, the adaptation is active and the parameters all move towards the correct values ($\eta = \zeta = g = f = 1$). They do not quite reach the correct value due to the lack of persistency of excitation but they all get near the

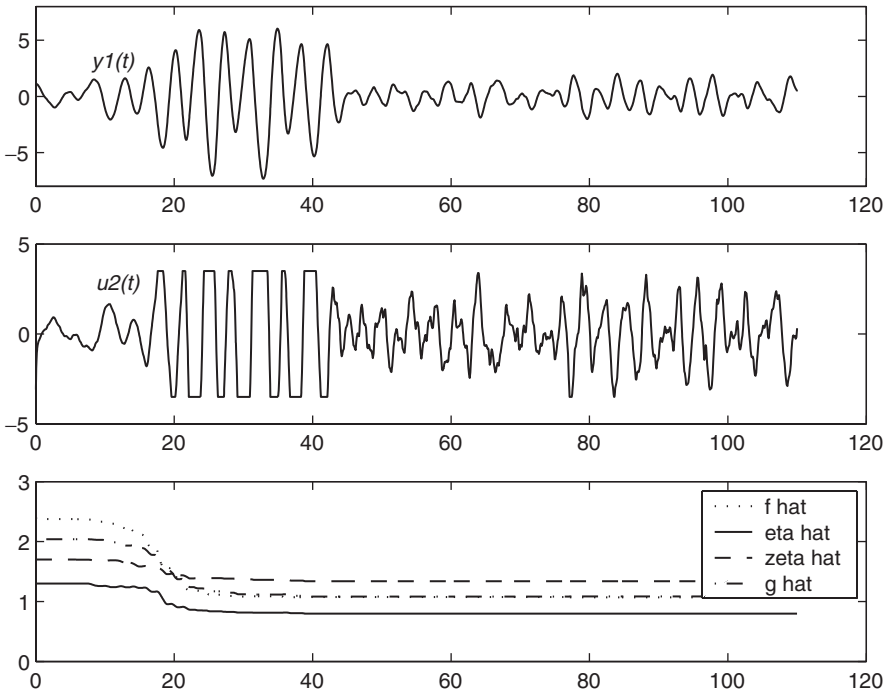

Fig. 3. Time traces of $y_1(t), u_2(t)$, and $\hat{\eta}(t), \hat{\zeta}(t), \hat{g}(t), \hat{f}(t)$.

value of 1. It is not necessary for the parameter estimates to reach the correct parameter value, it suffices for them to reach stabilizing values.

- In the third interval, 20–45 s, the controller is working hard at stabilizing the system, and it succeeds. The controller gets deeply into saturation. Without the saturation at 3.5, it would be applying control values on the order of 8.
- The fourth interval, after 45 s, shows the quasi-steady state of the system. The noise prevents the output from being zero but the output is not going unstable due to the action of the control. The adaptation seems to not be active any more. This is due to the deadzone. Since the estimation error does occasionally exceed $b = 0.06$, the parameters do drift, but extremely slowly. A burst after an extremely long period of time is possible. The length of this time can be controlled with the size of b.

One phenomenon that we do not show in the figure is that $y_1(t)$ and $y_2(t)$ are not symmetric, in a statistical, quantitative sense. They qualitatively behave similarly but most of the time $y_1(t)$ is larger than $y_2(t)$. This only happens in the presence of the deadzone. It might be puzzling that a perfectly symmetric plant with a perfectly symmetric controller, driven by symmetric noise, responds asymmetrically (even when the initial conditions are chosen symmetric). The explanation lies in the estimation algorithm. The parametric model used for designing adaptation is only the first of the two physical equations (31), which is given in (58) with the Pade approximation. This makes the entire feedback system respond differently to perturbations in y_1 versus those in y_2.

8. Conclusions

For a two-input–two-output LTI model with a time delay, which qualitatively fits both thermoacoustic combustor instabilities and compressor blade flutter instabilities in jet engines, we have designed an adaptive controller that simultaneously estimates the uncertain time delay and resonant modes. Our adaptive controller is a MIMO pole placement scheme with indirect adaptation. Instead reverting to a textbook linear parametrization, which would overparametrize the problem to avoid nonlinear parameter dependence, our scheme estimates only physical parameters. We present simulations in which, with the help of a deadzone in the adaptation law, our controller successfully stabilizes the uncertain system in the presence of noise and severe actuator saturation.

References

Ariyur, K. B., & Krstic, M. (2003). *Real time optimization by extremum-seeking control*. New York: Wiley.

Banaszuk, A., Ariyur, K. B., Krstic, M., & Jacobson, C. A. (2004). An adaptive algorithm for control of combustion instability. *Automatica*, *40*, 1965–1972.

Banaszuk, A., Hagen, G., Mehta, P., & Oppelstrup, J. (2003). A linear model for control of thermoacoustic instabilities on an annular domain. *Proceedings of the IEEE conference on decision and control*.

Candel, S. M. (1992). Combustion instabilities coupled by pressure waves and their active control. *Proceedings of the fourth international symposium on combustion*. The Combustion Institute (pp. 1277–1296).

Dasgupta, S. (1988). Adaptive identification of systems with polynomial parametrizations. *IEEE Transactions on Circuits and Systems*, *35*, 599–603.

Elliott, H., Wolovich, W. A., & Das, M. (1984). Arbitrary adaptive pole placement for linear multivariable systems. *IEEE Transactions on Automatic Control*, *29*, 221–228.

Limanond, S., & Tsakalis, K. S. (2001). Adaptive and non-adaptive 'pole-placement' control of multivariable linear time-varying plants. *International Journal of Control*, *74*, 507–523.

Ling, Y., & Tao, G. (1997). Adaptive backstepping control design for linear multivariable plants. *International Journal of Control*, *68*, 1289–1304.

Morse, P. M., & Ingard, K. U. (1968). *Theoretical acoustics*. Princeton University Press.

Seume, J. R., Vortmeyer, N., Krause, W., Hermann, J., Hantschk, C. -C., Zangl, P., Gleis, S., Vortmeyer, D., & Orthmann, A. (1997). Application of active combustion instability control to a heavy duty gas turbine. In *Proceedings of the ASME Asia '97 congress and exhibition*, Singapore, October 1997. ASME Paper 97-AA-119.

Sun, J. (1993). A multilinear model for parameter identification of partially known systems. *Proceeding of the 32nd conference on decision and control* (pp. 3040–3045).